

17C.4 Thermodynamic Structure and Evolution of the low level eye of Hurricane Lili (2002)

Paul A. Fuentes*

University of Hawaii, Honolulu, HI/WFO Key West, FL

Gary M. Barnes

University of Hawaii, Honolulu, HI

1. Introduction

Recently the concept of super-intensity has been argued (Persing and Montgomery 2003, Montgomery et al. 2006), where high-energy air residing in the eye can be entrained into the updrafts of the eyewall. This results in a more buoyant updraft and ultimately a more intense hurricane than what one would expect based on maximum potential intensity theory. Satellites reveal the presence of eddies in the eye that would promote the mixing of air from the eye to the eyewall (Kossin and Schubert 2004), and aircraft measurements show a relationship between vorticity and equivalent potential temperature (θ_e) radial profiles through the eye-eyewall region (Kossin and Eastin 2001). Such results stimulate us to explore the thermodynamic structure of the lower-eye of more hurricanes to identify repeatable features and determine if mixing between the eye and eyewall is frequent. If mixing between the eye and eyewall is apparent, is there a concurrent change in MSLP?

Forty-four Global Positioning System (GPS) dropwindsondes (sondes) were deployed in the eye of Lili from Sept. 29th through Oct. 3rd, 2002 by NOAA WP-3D and USAF C-130 aircraft. Forty-two of the forty-four sondes were deployed within 4 km of the circulation center and provide vertical profiles of temperature and moisture while flight level data, mostly at 700

*Corresponding author address: Paul A. Fuentes, National Weather Service, Key West Forecast Office, 1315 White Street, Key West, FL 33040; paul.fuentes@noaa.gov

hPa, provided radial profiles across the eye and eyewall. The sampling distribution encompassed tropical storm to category 4 intensities that captured periods of rapid intensification (18 m s^{-1} over 24 h), extreme rapid decay (23 m s^{-1} over 13 h) and steady state conditions while entirely over the Gulf of Mexico.

2. Data

The GPS sonde data were processed using the Atmospheric Sounding Processing Environment (ASPEN) software developed by NCAR. The processed data from ASPEN were also evaluated against an alternative processing method using the Editsonde software package developed at HRD. Comparisons of the forty-four sondes reveal only minor variations in temperature which were typically within the uncertainty error of the instrument. The relative humidity data also show minor variations with only two of the sondes showing differences slightly greater than 5%. The post-processed ASPEN data were further examined and corrected for additional sensor wetting errors addressed by Barnes (2008).



Figure 1. Distribution of forty-four GPS sondes in the eye of Lili during the period from Sept. 28th (2356 UTC) - Oct. 3rd (1203 UTC). Deployment of a GPS sonde denoted by a red diamond. NHC 6-h “best track” minimum central pressure (hPa, thin black line).

The sampling distribution of GPS sondes in the lower eye throughout the 4.5 day period typically show a 2 hour (h) interval between deployments on an individual flight with larger gaps of ~5-7 h between flights (Fig. 1). Flight level data from 38 passes through the approximate circulation center, typically at 700 hPa, were utilized in conjunction with GPS sonde data to examine thermodynamic variables in the lower eye and eyewall. A ten second resolution for the flight level data was chosen for the NOAA passes for consistency with the C-130 data which were only available at this coarser resolution. Sensor wetting errors were also addressed following the method of Zipser et al. (1981).

3. Analysis

The evolution of θ_e below 2.5 km in the eye shows an approximate linear increase of 16, 22 and 24 K at 10, 500 and 1000 m respectively from TS intensity through rapid decay (Fig. 2). A notable increase in energy that occurred during Lili's rapid decay phase can be seen in the progression of four θ_e profiles from Oct. 2-3rd (2139 UTC - 1203 UTC) (Fig. 3a) with an average layer increase of over 7 K through the 2 km layer (Fig 3b). Estimates of oceanic heat and moisture fluxes, derived using GPS sonde observations, reveal a flux time requirement of 50 h to realize the rapid energy increase witnessed during rapid decay. Additional periods when rapid energy increases in the lower eye occurred during steady state and weaker intensification periods also show conditions where oceanic moisture and heat fluxes are insufficient in explaining the observed increases thus requiring an additional energy source. A few periods that exhibited a sharp decrease in θ_e values in the lower eye also existed in Lili.

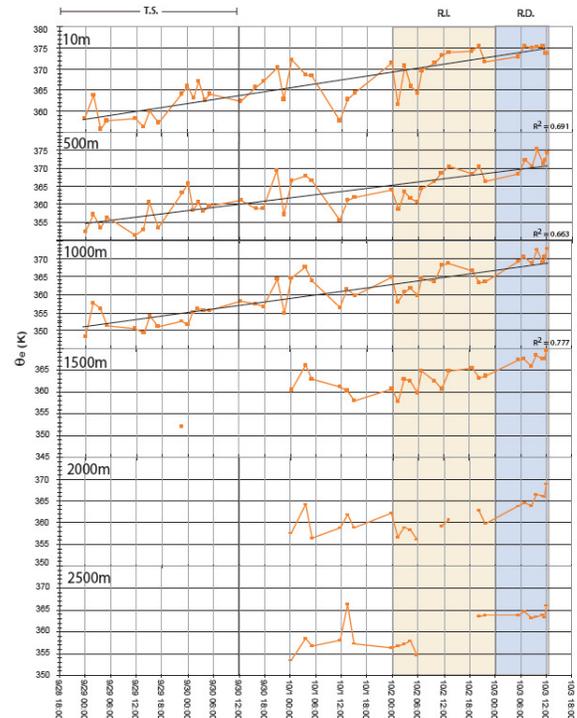


Figure 2. GPS sonde sample period from Sept. 28th (2356 UTC) - Oct. 3rd (1203 UTC) equivalent potential temperature (K) at 10 m, 100 m, 500 m, 1 km, 1.5 km, 2 km and 2.5km altitude. Data voids above 1.5 km reflect profiles with data initiating below 1.5 km. Thin black line indicates the best fit trend for a linear regression at 10 m, 500 m, and 1km. Periods of rapid intensification (R.I.) and decay (R.D.) denoted by tan and light blue columns respectively. Tropical Storm intensity denoted by black line and T.S. brackets

The most notable period occurred on Oct. 1st from 0333 to 1140 UTC when an average layer decrease of ~8 K occurred below 2.5 km (Fig. 4). During this period the eye diameter contracted which would imply a displacement of mass from the low level eye to the eyewall and would result in an exchange of high θ_e air from the inner eye with the eyewall as well. A less prominent decrease in the lower eye of ~0.5 K in the lower 2 km (not shown) occurred during the last 12 h of rapid intensification along with a ~3 K θ_e increase in the eyewall. Additionally, a 6

h period at the start of RI also denoted a period where average values of θ_e below 1 km were decreasing concurrently with increasing eyewall values.

Flight level radial thermodynamic profiles exhibit notable change with intensity in which increases in θ_e in the eyewall precede increases in the eye (Fig. 5). Periods when θ_e values are elevated in the eyewall and depressed in the eye occur during rapid intensification and exhibit a transition to flatter gradients across the eyewall during steady state and decay phases.

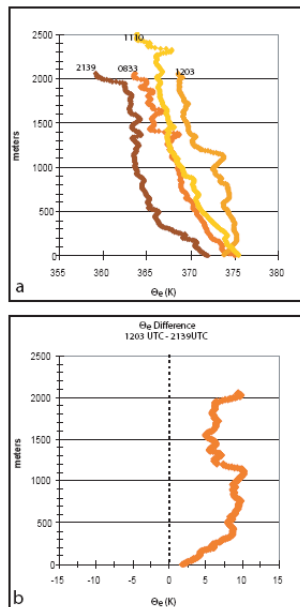


Figure 3. Profiles of equivalent potential temperature (K) from the GPS dropwindsonde in the lower eye of Hurricane Lili at: a) 10/2 - 2139 UTC, 10/3 - 0833, 1110, 1203 UTC. b) θ_e difference between 10/3 at 1203 UTC and 10/2 at 2139 UTC. Zero line marked as a dashed black line.

The vertical thermodynamic structure during steady state and decaying periods in Lili also demonstrate cooling and moistening of the lower eye subsequent to periods of rapid intensification. The previously discussed sharp decrease in θ_e in the lower eye on Oct. 1st was also coincident with a 4 to 5 K increase in the eyewall θ_e values estimated from flight

level data. The increased values observed in the eyewall do not exceed the initial values in the lower eye before the sharp decrease occurred allowing the eye to be a potential source for the increases in the eyewall. This abrupt decrease of θ_e in the eye and coincident jump in the eyewall is thought to have occurred via mixing from the eye to the eyewall although any influence on lowering MSLP may have been small as Lili's MSLP deepened less than 3 hPa during these eight hours. The diminished θ_e in the eye seen during RI may also have been due to exchanges between the eye and eyewall. These periods did not show a sharp decrease of θ_e in the eye and increase in the eyewall like that seen on Oct. 1st.

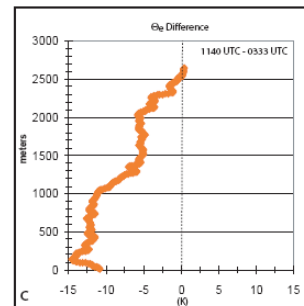


Figure 4. θ_e difference between 1140 UTC and 0333 UTC, Oct. 1st, 2002. Zero line marked as a dashed black line.

4. Discussion

A plausible explanation for the observed vertical and radial thermodynamic structural changes is that the increase in θ_e in the lower eye is a result of episodic exchanges between the lower eye and eyewall, supporting the arguments of Kossin and Eastin (2001) and is depicted in the conceptual model in figure 6. Increases in θ_e in the eyewall precede increases in the eye and show a cyclical structure change from elevated θ_e values in the eyewall and depressed values in the eye during intensification periods to a flat gradient across the eye

and eyewall during steady or weakening periods.

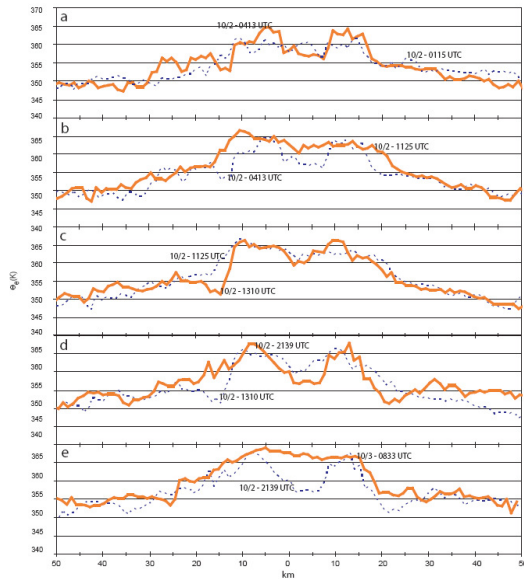


Figure 5. 700 hPa 10 second flight level data overlays of equivalent potential temperature (K) with distance from the circulation center (km). The earlier profile is shown with a dashed blue line and the later profile shown in orange for periods on October 2, 2002 at: a) 0115 UTC and 0413 UTC b) 0413 UTC and 1125 UTC c) 1125 UTC and 1310 UTC d) 1310 UTC and 2139 UTC e) 2139 UTC and 10/3 at 0833 UTC.

During periods when the convection in the eyewall has weakened, some of the inflow does not ascend in the eyewall but instead penetrates into the eye where it remains to collect additional oceanic heat fluxes and builds a reservoir of high θ_e air.

In Lili, there was a steady increase of θ_e in the lower eye in which contributions from surface fluxes were not sufficient in explaining the observed increase during intensifying, steady state, and decaying phases of its evolution. This steady increase of θ_e saw shorter periods defined by a simultaneous decrease of θ_e in the lower eye and an increase in the eyewall. These three periods all occurred during intensification but with differing

magnitudes. The most prominent case of decreasing θ_e in the lower eye and increasing values in the eyewall also had the smallest drop in MSLP during the observed period. Low-level exchanges in Lili likely occurred between the eye and eyewall and may have contributed to a portion of the observed decrease in MSLP.

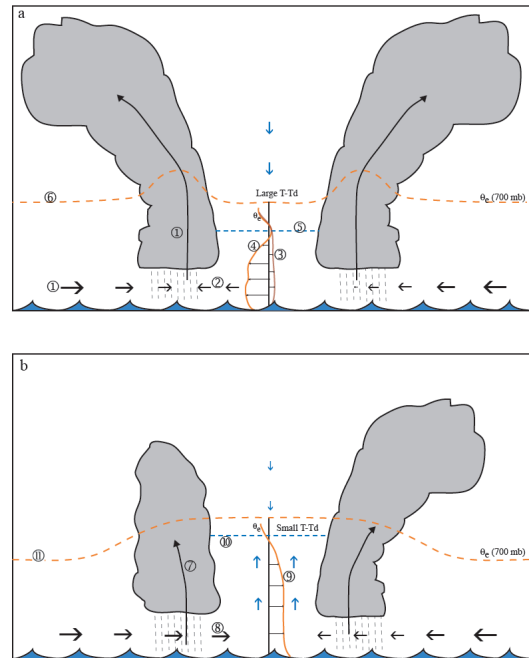


Figure 6. A depiction of episodic exchanges between the lower eye and eyewall and the resultant changes in the vertical and radial thermodynamic structure. a) Represents a period of strong convection in the eyewall and the incorporation of θ_e from the lower eye to the eyewall. b) Represents a period of weakened convection in the eyewall with minimal exchange between the eyewall to the eye or transport from the eye to eyewall.

Numbers indicate:

- 1- Low-level inflow ingested into eyewall convection with vigorous updrafts
- 2- Mass transport from the eye to the eyewall may occur
- 3- Vertical profile of θ_e with minimal exchange between the eye and eyewall
- 4- Vertical profile of θ_e when transport from the eye to the eyewall has occurred
- 5- Lowering inversion base if mass is transported from the eye to the eyewall forcing subsidence above

- 6- Radial profile of θ_e at 700 hPa showing double hump structure in the eyewall
- 7- Weakened eyewall convection
- 8- Weakened eyewall convection allowing more inflow to penetrate the eye
- 9- Vertical profile of θ_e increasing in the lower eye
- 10- Rising inversion level
- 11- Radial profile of θ_e becomes flatter across

5. References

Barnes, G. M., 2008: Atypical thermodynamic profiles in hurricanes. *Mon. Wea. Rev.*, **136**, 631-643.

Kossin, J. P., and M. D. Eastin, 2001: Two distinct regimes in the kinematic and thermodynamic structure of the hurricane eye and eyewall. *J. Atmos. Sci.*, **58**, 1079–1090.

_____, B.D. McNoldy, and W.H. Schubert, 2002: Vortical Swirls in Hurricane Eye Clouds. *Mon. Wea. Rev.*, **130**, 3144–3149.

Persing, J., and M.T. Montgomery, 2003: Hurricane Superintensity. *J. Atmos. Sci.*, **60**, 2349–2371.

Montgomery, M.T., M.M. Bell, S.D. Aberson, and M.L. Black, 2006: Hurricane Isabel (2003): New Insights into the Physics of Intense Storms. Part I: Mean Vortex Structure and Maximum Intensity Estimates. *Bull. Amer. Meteor. Soc.*, **87**, 1335–1347.

Zipser, E.J., R.J. Meitín, and M.A. LeMone, 1981: Mesoscale Motion Fields Associated with a Slowly Moving GATE Convective Band. *J. Atmos. Sci.* **38**, 1725-1750